

Structural Health Monitoring of CFRP Propellers by Piezoelectric Line Sensors

RYOTA HAMADA, TAKAFUMI OGURA, SHOGO FUJITA,
HIDEAKI MURAYAMA, TOSHIO YAMATOI,
TOSHIYUKI INOUE, KAZUYA HAYASHI, MAI TAKAHARA,
KENTARO GOTO and KOTARO FURUKAWA

ABSTRACT

Recently, marine propellers made of carbon fiber reinforced plastics (CFRP) have been put into practical use for merchant ships. CFRP have advantages of high specific stiffness/strength and vibration damping property, and these can reduce the weight and noise of propellers to increase the efficiency and comfort in operation. However, they are more susceptible to impact or cavitation that cause critical damage than conventional propellers made of a copper alloy. Therefore, it can improve the reliability of CFRP propellers to assess the structural integrity based on structural health monitoring (SHM). In this study, piezoelectric line sensors were embedded into intact and damaged blades, respectively, in CFRP propellers with which a leisure boat was equipped. We could successfully detect vibration deformation of the propellers during the boat was moving, and we found that the amplitudes of the measured signals in the damaged blades were larger than those in the intact ones. Consequently, we can say that the applicability of the embedded piezoelectric sensors to SHM system for marine propellers is shown and it will increase the reliability not only of the propellers but also of the ship operation in the sea.

INTRODUCTION

High-strength brass castings and nickel-aluminum bronze castings (NAB) have been commonly used as materials for marine propellers. However, the minable life of copper is shorter than other base metals, such as iron and aluminum, that can be used for structural materials, while its consumption is increasing because of the recent electrification of vehicles. In result, the price of copper has soared in recent years, raising concerns about the supply of copper for the marine propellers.

When it comes to replace the conventional material for marine propellers, carbon fiber reinforced plastics (CFRP) can be an attractive candidate because of their advantages of high specific stiffness/strength and vibration damping property that can reduce the weight and noise of the propellers to increase the efficiency and comfort in operation. Yamatogi and et al., have developed CFRP propellers for merchant ships and have confirmed they improve the efficiency and suppress the vibration in operation [1,2].

However, CFRP is less resistant to cavitation erosion than NAB [3]. As a result, the surface of the CFPR blades can be scratched to cause critical damage [3]. In order to improve applicability of CFRP propellers to large vessels, SHM technology to detect damage and deterioration is able to play a significant role. Fiber optic sensors and piezoelectric sensors that can be embedded in structures have been mainly used to SHM of composite materials.

In the composite manufacturing process, the resin flow was monitored using a distributed strain-sensing method during the VaRTM (Vacuum Resin Transfer

Ryota Hamada, Takafumi Ogura, Shogo Fujita, Hideaki Murayama, The University of Tokyo, Tokyo, Japan. Email: ryota-hamada-2018@g.ecc.u-tokyo.ac.jp

Toshio Yamatogi, Toshiyuki Inoue, Kazuya Hayashi, Mai Takahara, Nakashima Propeller Co., Ltd., Okayama, Japan.

Kentaro Goto, Kotaro Furukawa, Hongo Development Group Inc., Tokyo, Japan.

Molding) [4]. Composite propeller blades in which embedded arrays of FBG sensors were recorded the dynamic strains experienced by those blades during water tunnel testing [5]. A waterproof strain gauge was attached in the bronze propeller blades under water tunnel test, and dynamic strain was measured in non-uniform flow [6]. FBG sensors was embedded in a hull made of composite materials, and temperature and strain distributions along the FBG sensor were measured [7]. Composite structures with embedded piezoelectric sensors have been developed and vibration measurements were conducted [8,9]. A feasibility evaluation of composite propellers with embedded piezoelectric line sensors has been conducted [10]. To embed fiber optic sensors on marine propellers that rotate underwater, miniaturization and power saving of interrogator and robustness of monitoring system are required. On the other hand, piezoelectric sensors are simpler systems and less power consumption than fiber optic sensors. Furthermore, piezoelectric line sensors are easily embedded in composite structures and able to measure mean strain distribution that cannot be measured with strain gauges. Therefore, we considered SHM of propellers using piezoelectric line sensors.

In this study, we conducted two experiments. Firstly, we attached a strain gauge and a piezoelectric line sensor on a cantilever beam. We generated free vibration in the beam and measured strain and strain-rate by the strain gauge and the piezoelectric sensor, respectively. We found the voltage-to-strain-rate conversion coefficient by comparing the result of the strain gauge with that of the piezoelectric line sensor. Secondly, we embedded piezoelectric line sensors into intact and damaged blades, respectively, in CFRP propellers with which a leisure fishing boat was equipped. By applying the obtained conversion coefficient to the voltage of the embedded piezoelectric line sensors, we successfully detected the variation of the strain rate of the propeller blades during the boat was moving.

VIBRATION MEASUREMENTS OF A CANTILEVER BEAM

In this chapter, we discuss the results of experiments conducted to investigate the characteristics of piezoelectric line sensors used for boat propeller monitoring.

The piezoelectric line sensors used in this study consist of three parts: an inner conductor, an insulator covering the inner conductor, and an outer conductor wrapped around the insulator [11]. Piezoelectric lines are characterized by the fact that when tension is applied, they output a charge proportional to the tension [11, 12].

Next, we describe the processes and results of the cantilever free vibration test. As shown in Fig. 1, we prepared a cantilever with a clamped fixed end and a free end.

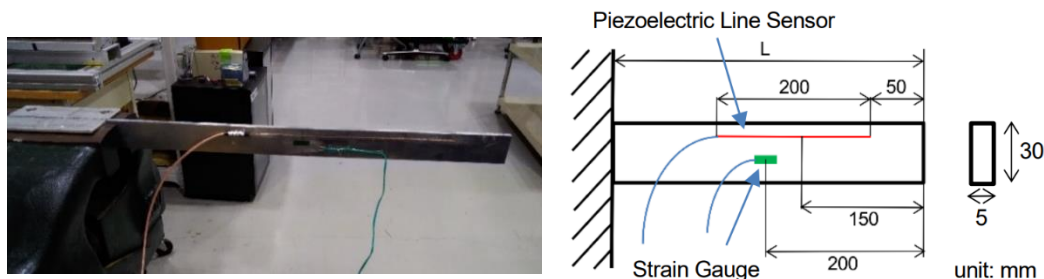


Figure 1. Cantilever with sensors.

The cantilever is made of an aluminum alloy and has a width of 30 mm and a thickness of 5 mm. We changed the position of the fixed end and thus set the cantilever length L in 5 steps: 500 mm, 450 mm, 400 mm, 350 mm, and 300 mm. By varying the natural frequency of the beam and measuring different amplitudes, we confirmed that the sensor can be used to detect different amplitudes for intact and damaged blades. A strain gauge was bonded 200 mm at a position away from the free end, and a piezoelectric line sensor with 200 mm in length was bonded from a position 50 mm away from the free end, as show in Fig. 1. Output voltages of the strain gauge and the piezoelectric sensors were obtained from an AD converter at the sampling rate of 1 kHz. The free end was slightly bent by fingers and released to induce free vibration.

We converted the voltage V_{sg} measured by the strain gauge to the strain ε_{sg} at the installation position of the strain gauge. Figure 2 shows ε_{sg} and the voltage of the piezoelectric line sensor V_{pl} when beam lengths is 500 mm or 300 mm, respectively. There is a phase difference between ε_{sg} and V_{pl} . Figure 3 shows the FFT analysis results of ε_{sg} and V_{pl} . V_{pl} contained low frequency components around 0 Hz.

A strain gauge is located 200 mm from the free end, and the center of the piezoelectric line sensor embedded section is located 150 mm from the free end. Since the strain distribution in the longitudinal direction of the beam is linear, the strain ε_{pl} at the center of the piezoelectric line sensor embedded section is expressed by

$$\varepsilon_{pl} = \frac{150}{200} \varepsilon_{sg}. \quad (1)$$

We compared V_{pl} with the strain rate $\frac{d\varepsilon_{pl}}{dt}$ obtained by time-differentiating ε_{pl} . From the FFT analysis results, we found that the waveforms of $\frac{d\varepsilon_{pl}}{dt}$ and V_{pl} contain low frequency components around 0 Hz and high frequency components after the first natural frequency, so that we applied 10 Hz to 50 Hz band-pass filters to $\frac{d\varepsilon_{pl}}{dt}$ and V_{pl} . Figure 4 shows the results of 500 mm and 300 mm.

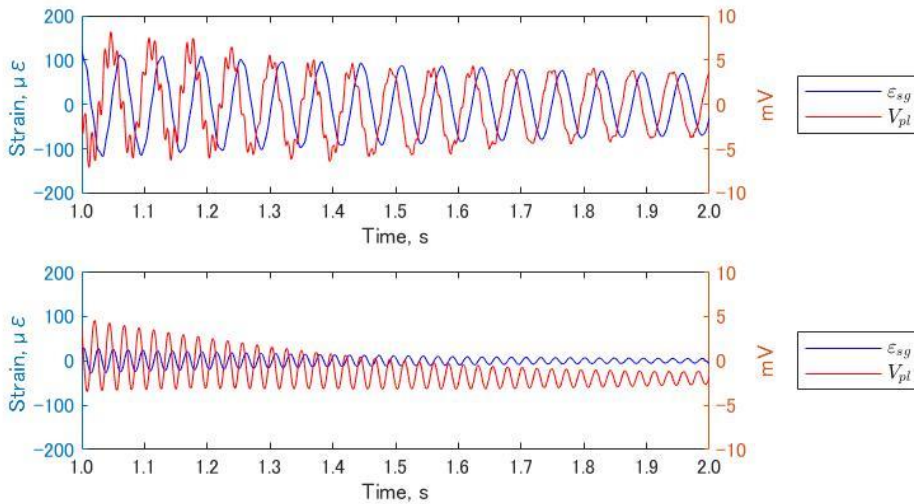


Figure 2. ε_{sg} and V_{pl} when beam length is 500 mm (top) and 300 mm (bottom).

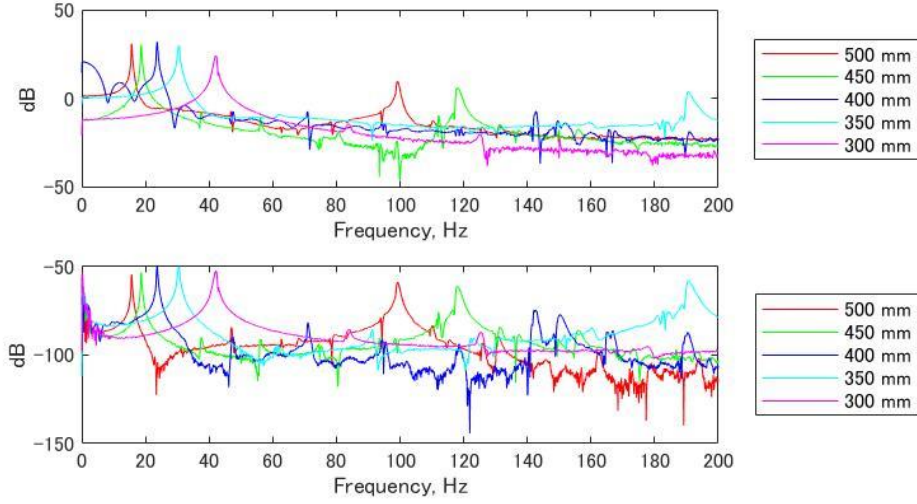


Figure 3. FFT analysis results of ε_{sg} (top) and V_{pl} (bottom) for each beam length.

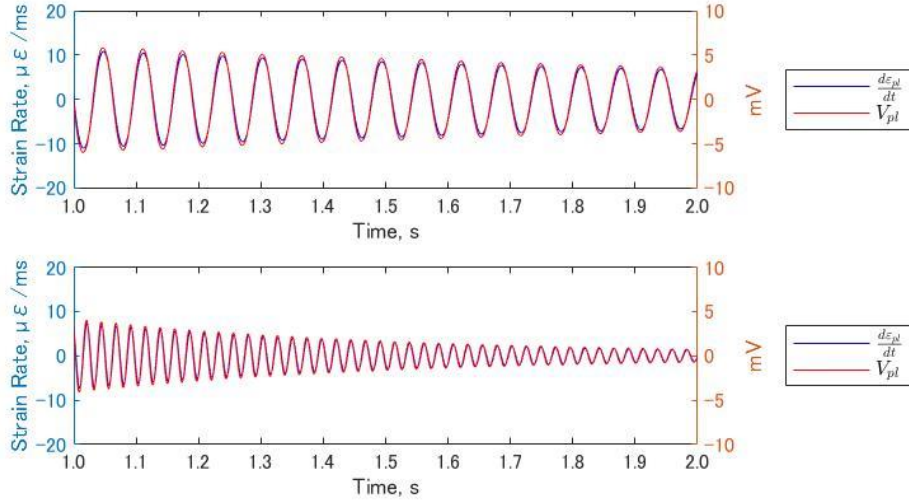


Figure 4. Filtered results of $\frac{d\varepsilon_{pl}}{dt}$ and V_{pl} when beam length is 500 mm (top) and 300 mm (bottom).

From Fig. 4, it can be said that $\frac{d\varepsilon_{pl}}{dt}$ and V_{pl} are in a proportional relationship. Thus, it can be expressed as

$$\frac{d\varepsilon_{pl}}{dt} = cV_{pl}, \quad (2)$$

where c [$\mu\varepsilon/V \cdot ms$] is the conversion coefficient.

By calculating the effective value of $\frac{d\varepsilon_{pl}}{dt}$ and V_{pl} with Root Mean Square (RMS) as

$$c = \frac{eff\left(\frac{d\varepsilon_{pl}}{dt}\right)}{eff(V_{pl})}, \quad (3)$$

conversion coefficient c for each of the five lengths as shown in Table I can be derived.

TABLE I. CONVERSION COEFFICIENT FOR BEAM LENGTH.

L [mm]	500	450	400	350	300
c [$\mu\epsilon/V \cdot ms$]	1834	1863	1859	1837	1833

By averaging these values, c of the piezoelectric line sensors used for the propeller monitoring is given by

$$c = 1.8 \times 10^3 [\mu\epsilon/V \cdot ms]. \quad (4)$$

By applying the obtained c to V_{pl} , we were able to show that the strain rate derived from the strain gauge and the strain rate calculated from the piezoelectric line sensor match.

STRUCTURAL HEALTH MONITORING OF PROPELLERS

In this chapter, we describe SHM results for propeller blades using piezoelectric line sensors. Figure 5 shows the leisure fishing boat and CFRP propeller used in the experiment.

The dimension of the boat is $10.50 \text{ m} \times 2.75 \text{ m} \times 1.4 \text{ m}$ and the gross tonnage is 3.3 G/T. The boat has a 6-cylinder, 4-stroke engine with a maximum output of 300 PS and a reduction ratio of 2.58. The propeller used in the test is made of quasi-isotropic CFRP, which is made of carbon fiber and epoxy resin and formed by VaRTM. The propeller has a diameter of 680 mm and three blades. We tested two propellers with the same original blade shapes, one with all three intact blades and the other with all three damaged blades. As shown in Fig. 5, the damaged blades have chipped edges.

Piezoelectric line sensors were embedded on the propeller blade surface to measure the voltage generated when the propeller blade deformed. Piezoelectric lines with 200 mm in length and coaxial cable with MCX connector terminal specification at one end of the coaxial cable were used. Piezoelectric lines were placed on the suction surfaces of two leading and trailing edges out of three intact blades (i-Blade) and one leading



Figure 5. Leisure fishing boat (left) and CFRP propeller blades with embedded sensors and damage (right).

edge and trailing edge of three damaged blades (d-Blade). When embedding, black grooves as shown in Fig. 5 were carved in the blade surface, and the piezoelectric lines were embedded and then sealed with two-component epoxy resin adhesives. A donut-shaped watertight container made of ABS resin was fixed to the rotating shaft, a power source and a voltage measurement module composed of data logger and AD converter were installed in it. The piezoelectric lines of each blade were connected to the watertight container by coaxial cables. The measured data were taken out from the module after the experiment.

In this monitoring test, the piezoelectric line signal was measured while navigating the actual sea area at multiple speeds. During cruising, the output was adjusted so that the engine speed was set in advance while visually checking the engine speed. The voltage of each piezoelectric line was recorded in the range of -2.5 V to 2.5 V at a sampling rate of 1 kHz .

Among the measured signals, Fig. 6 shows the DC component removed signals at a propeller speed of around 600 rpm for intact and damaged blades. However, the sensor at the trailing edge of the i-Blade (Blade 2) could not be measured because the coaxial cable was damaged. Since it has three blades, there is a phase shift of about 120° between blades.

As shown in Fig. 7, the FFT analysis revealed a peak near 10 Hz that coincided with the propeller rotation speed of 600 rpm .

Figure 8 shows the result of applying a 15 Hz low-pass filter to the signal and applying the conversion coefficient c given by equation (5). The amplitudes of the strain rate of the damaged blades were about twice as large as those of the intact blades, suggesting that the bending stiffness of the blades decreased due to the damage, resulting in large deformation. Moreover, from Fig. 7, the amplitude of the strain rate at the trailing edge is larger than that at the leading edge for the same blade. This indicates that the rotating blade deformation is larger at the trailing edge.

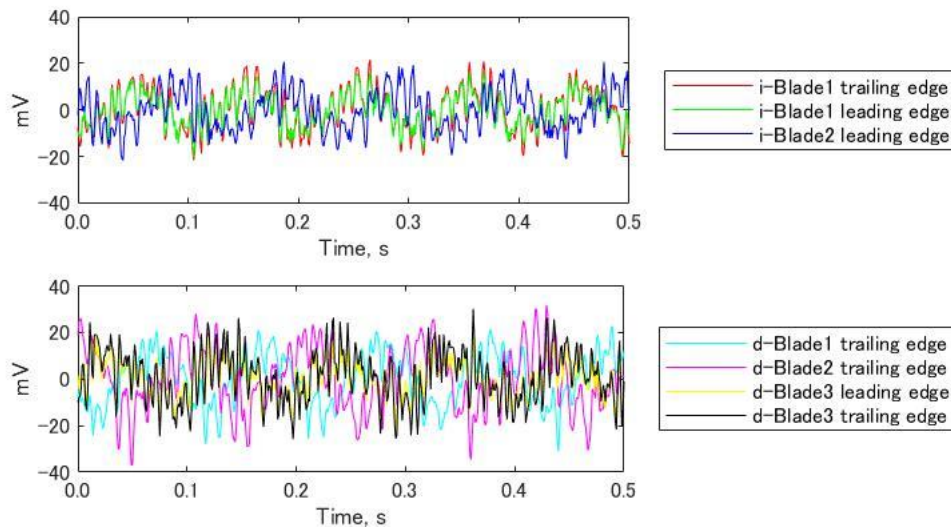


Figure 6. Signals of the intact blades of 601 rpm (top) and damaged blades of 581 rpm (bottom).

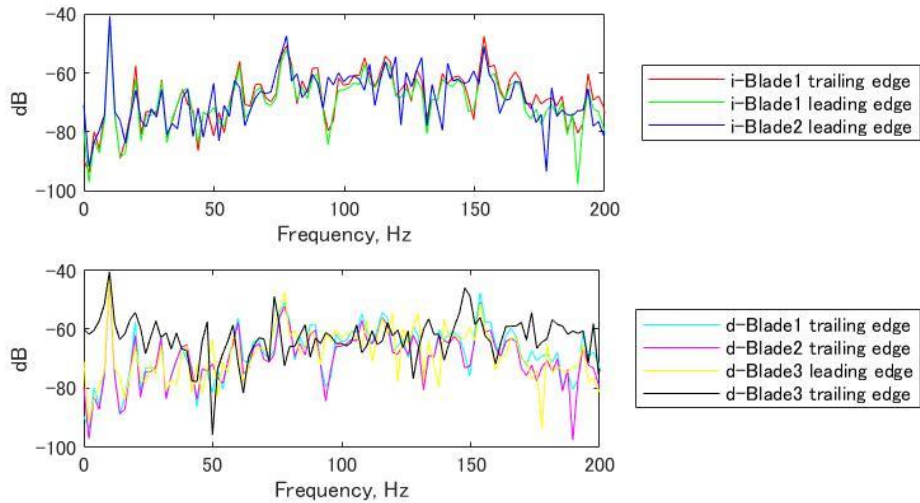


Figure 7. FFT analysis results of the intact blades of 601 rpm (top) and damaged blades of 581 rpm (bottom).

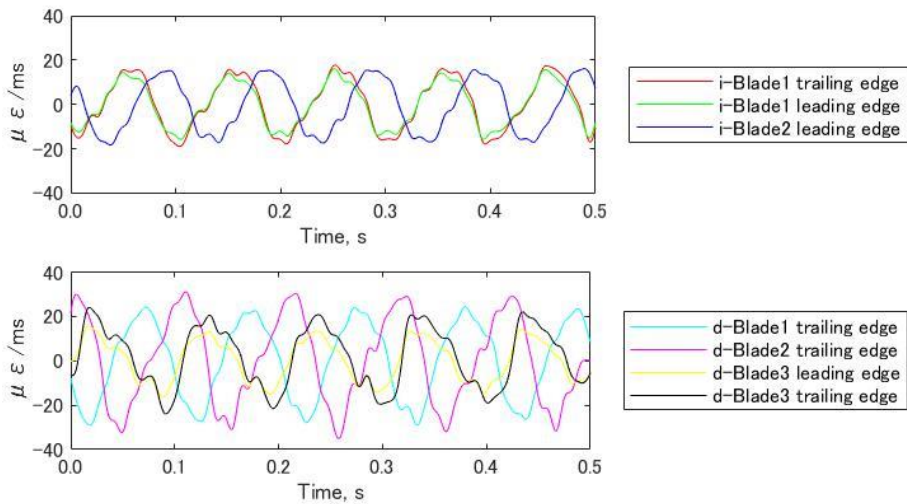


Figure 8. Strain rates of the intact blades of 601 rpm (top) and damaged blades of 581 rpm (bottom).

CONCLUSIONS

In this study, we successfully detected the strain rate of marine propeller blades rotating in the sea using piezoelectric line sensors.

Firstly, a free vibration test of a cantilever with a piezoelectric line sensor was carried out, and the coefficient that converts the voltage of the piezoelectric line into the strain rate was obtained from the comparison with the measurement result of the strain gauge.

Secondly, we installed piezoelectric line sensors on the intact and damaged blades of CFRP propellers of a leisure fishing boat, and measured the voltage generated at the leading and trailing edges. By applying the obtained conversion coefficient to the measured voltage, the strain rate generated in the rotating propeller was derived.

In the future, we have a plan to realize real-time propeller monitoring and optimize the sensor arrangement by comparing with the fluid-structure interaction (FSI) analysis of propellers.

ACKNOWLEDGEMENT

This research was supported by the Ministry of Internal Affairs and Communications SCOPE, Japan [Grant: JP215003003]. The authors would also like to thank Dr. Yoshida of Mitsui Chemicals, Inc. for technical advice on piezoelectric line sensors.

REFERENCES

1. Toshio Yamatogi, Hideaki Murayama, Kiyoshi Uzawa, Takahiro Mishima and Yasuaki Ishihara. 2011. "Study on Composite Material Marine Propellers," *Journal of The Japan Institute of Marine Engineering.*, 46:330-340.
2. Toshio Yamatogi. 2016. "Development of the Carbon Composite Marine Propeller Realizing Energy Saving," *Seikei-Kakou.*, 28(12):490-494.
3. Toshio Yamatogi, Hideaki Murayama, Kiyoshi Uzawa, Kazuro Kageyama and Naoki Watanabe. "Study on cavitation erosion of composite materials for marine propeller," presented at the ICCM International Conferences on Composite Materials, 2009.
4. Jae-Moon Jeong, Soohyun Eum, Seung Yoon On, Kazuro Kageyama, Hideaki Murayama, Kiyoshi Uzawa and Seong Su Kim. 2022. "In-situ resin flow monitoring in VaRTM process by using optical frequency domain reflectometry and long-gauge FBG sensors," *Composite Structures.* 282:115034.
5. Mark Seaver, Stephen T. Trickey, and Jonathan M. Nichols. 2006. "Strain Measurements from FBGs Embedded in Rotating Composite Propeller Blades," *Optical Fiber Sensors.* OSA Technical Digest (CD) (Optica Publishing Group). paper ThD2.
6. Jin Tian, Paul Croaker, Zhiyi Zhang and Hongxing Hua. 2016. "Dynamic strain measurements of marine propellers under non-uniform inflow." *Journal of Physics: Conference Series.* 744.
7. Magdalena Mieloszyk, Katarzyna Majewska and Wieslaw Ostachowicz. 2021. "Application of embedded fibre Bragg grating sensors for structural health monitoring of complex composite structures for marine applications." *Marine Structures.* 76:102903.
8. Mehrdad N. Ghasemi-Nejhad, Richard Russ and Saeid Pourjalali. 2005. "Manufacturing and Testing of Active Composite Panels with Embedded Piezoelectric Sensors and Actuators." *Journal of Intelligent Material Systems and Structures - J INTEL MAT SYST STRUCT.* 16:319-333.
9. Robert Schulze, Petra Streit, Thomas Fischer, Alexander Tsapkolenko, Michael Heinrich, Martynas Sborikas, Kroll, L., Gessner, T. and Michael Wegener. 2014. "Fiber-reinforced composite structures with embedded piezoelectric sensors." *Proceedings of IEEE Sensors.* 2014. 1563-1566.
10. Arnaud Huijjer, Xiaobo Zhang, Christos Kassapoglou and Lotfollah Pahlavan. 2022. "Feasibility evaluation for development of composite propellers with embedded piezoelectric sensors." *Marine Structures.* 84:103231.
11. Mitsunobu Yoshida, Katsuki Onishi, Kazuhiro Tanimoto and Shigeo Nishikawa. 2017. "Flexible tension sensor based on poly(l-lactic acid) film with coaxial structure." *Japanese Journal of Applied Physics.* 56:10PG02.
12. Jayant Sirohi and Inderjit Chopra. 2000. "Fundamental Understanding of Piezoelectric Strain Sensors." *Journal of Intelligent Material Systems and Structures - J INTEL MAT SYST STRUCT.* 11:246-257.